J|A|C|S
ARTICLES
Published on Web 03/23/2006

Triple-Ion Interactions for the Construction of Supramolecular Capsules

Gennady V. Oshovsky, David N. Reinhoudt, and Willem Verboom*

Contribution from the Laboratory of Supramolecular Chemistry and Technology, MESA+ Research Institute for Nanotechnology, University of Twente, P.O. Box 217, 7500 AE Enschede, The Netherlands

Received January 12, 2006; E-mail: W.Verboom@utwente.nl

Abstract: A novel type of [2+4] capsules based on triple-ion interactions was obtained. Four monovalent anions (bromide, nitrate, acetate, and tosylate) bring together two tetrakis(pyridiniummethyl)tetramethyl cavitands by pyridinium−anion−pyridinium interactions. ESI-MS experiments have confirmed the capsule structure due to different fragmentation pathways of triple ions, cations, and ion-pairs. Each capsule encapsulates one or two anions, depending on its size. The capsules exist in equilibrium with hemicapsules containing three walls. The latter form complexes with phenols and anilines to give new unsymmetrical capsules containing both pyridinium−anion−pyridinium and pyridinium−guest−pyridinium walls.

Introduction

Self-assembled architectures such as capsules,[1] cages,[2] rosettes,[3,4] guanosine quartets,[5] metallacycles,[6] etc. are currently of interest in supramolecular chemistry.[3,7] Capsules are spherical molecules that are formed by specific interactions of two functionalized half-spheres. Due to multivalent interactions,[8] preferential formation of capsules takes place, while no polymerization is observed. The groups of Rebek and Böhmer systematically studied capsules on the basis of hydrogen-bonding interactions and their host−guest complexes.[1,9] A number of capsules have been obtained using metal−ligand[10] or electrostatic interactions.[11,12] However, to the best of our knowledge, triple-ion interactions have never been used to build capsules or any other type of supramolecular architectures.

Scheme 1. Formation of Triple Ions[a]

$$A^- + C^+ \rightleftharpoons AC$$

$$A^- + AC \rightleftharpoons ACA^-$$

$$C^+ + AC \rightleftharpoons CAC^+$$

[a] A^- = anion; C^+ = cation.

The formation of triple ions, the result of the interaction of a singly charged anion A^- or a cation C^+ with an ion-pair AC (Scheme 1), was proposed by Fuoss and Kraus more than 70 years ago.[13] Since that time, a variety of triple ions based on inorganic and organic ions have been studied not only in noncompetitive solvents (such as tetrahydrofuran, ethyl acetate, and chloroform)[14] but also in acetonitrile,[15] alcohols,[16] and even supercritical water.[17] These transient ionic intermediates, which are present in conducting electrolyte solutions, have been studied not only by a variety of electrochemical methods[13−16] but also by mass spectrometry.[18] Modern theories considering the properties of electrolyte solutions take into account the presence of triple ions and higher aggregates.[19]

Although the triple-ion concept originally comes from electrochemistry, coordination chemistry gives another view on these associates: there are two valencies, the charge of the ion

(1) Rebek, J. *Angew. Chem., Int. Ed.* **2005**, *44*, 2068−2078.
(2) Fujita, M.; Tominaga, M.; Hori, A.; Therrien, B. *Acc. Chem. Res.* **2005**, *38*, 369−378. Takeda, N.; Umemoto, K.; Yamaguchi, K.; Fujita, M. *Nature* **1999**, *398*, 794−796.
(3) Reinhoudt, D. N.; Crego-Calama, M. *Science* **2002**, *295*, 2403−2407.
(4) Prins, L. J.; De Jong, F.; Timmerman, P.; Reinhoudt, D. N. *Nature* **2000**, *408*, 181−184. Prins, L. J.; Huskens, J.; De Jong, F.; Timmerman, P.; Reinhoudt, D. N. *Nature* **1999**, *398*, 498−502.
(5) Davis, J. T. *Angew. Chem., Int. Ed.* **2004**, *43*, 668−698.
(6) Grote, Z.; Scopelliti, R.; Severin, K. *J. Am. Chem. Soc.* **2004**, *126*, 16959−16972.
(7) Lehn, J.-M. *Science* **2002**, *295*, 2400−2403. Whitesides, G. M.; Grzybowski, B. *Science* **2002**, *295*, 2418−2421.
(8) Badjić, J. D.; Nelson, A.; Cantrill, S. J.; Turnbull, W. B.; Stoddart, J. F. *Acc. Chem. Res.* **2005**, *38*, 723−732. Mammen, M.; Choi, S. K.; Whitesides, G. M. *Angew. Chem., Int. Ed.* **1998**, *37*, 2755−2794. Mulder, A.; Huskens, J.; Reinhoudt, D. N. *Org. Biomol. Chem.* **2004**, *2*, 3409−3424.
(9) Böhmer, V.; Vysotsky, M. O. *Aust. J. Chem.* **2001**, *54*, 671−677.
(10) Baldini, L.; Ballester, P.; Casnati, A.; Gomila, R. M.; Hunter, C. A.; Sansone, F.; Ungaro, R. *J. Am. Chem. Soc.* **2003**, *125*, 14181−14189. Haino, T.; Kobayashi, M.; Chikaraishi, M.; Fukazawa, Y. *Chem. Commun.* **2005**, 2321−2323. Pinalli, R.; Cristini, V.; Sottili, V.; Geremia, S.; Campagnolo, M.; Caneschi, A.; Dalcanale, E. *J. Am. Chem. Soc.* **2004**, *126*, 6516−6517; Zuccaccia, D.; Pirondini, L.; Pinalli, R.; Dalcanale, E.; Macchioni, A. *J. Am. Chem. Soc.* **2005**, *127*, 7025−7032.
(11) Corbellini, F.; Di Costanzo, L.; Crego-Calama, M.; Geremia, S.; Reinhoudt, D. N. *J. Am. Chem. Soc.* **2003**, *125*, 9946−9947. Corbellini, F.; Knegtel, R. M. A.; Grootenhuis, P. D. J.; Crego-Calama, M.; Reinhoudt, D. N. *Chem. Eur. J.* **2005**, *11*, 298−307. Zadmard, R.; Kraft, A.; Schrader, T.; Linne, U. *Chem. Eur. J.* **2004**, *10*, 4233−4239.
(12) Zadmard, R.; Junkers, M.; Schrader, T.; Grawe, T.; Kraft, A. *J. Org. Chem.* **2003**, *68*, 6511−6521.
(13) Fuoss, R. M.; Kraus, C. A. *J. Am. Chem. Soc.* **1933**, *55*, 2387−2399.
(14) Chen, Z. D.; Hojo, M. *J. Phys. Chem. B* **1997**, *101*, 10896−10902. Reich, H. J.; Sikorski, W. H.; Gudmundsson, B. O.; Dykstra, R. R. *J. Am. Chem. Soc.* **1998**, *120*, 4035−4036.
(15) Hojo, M.; Takiguchi, T.; Hagiwara, M.; Nagai, H.; Imai, Y. *J. Phys. Chem.* **1989**, *93*, 955−961.
(16) Hojo, M.; Fujime, C.; Yoneda, H. *Chem. Lett.* **1993**, 37−40.
(17) Oelkers, E. H.; Helgeson, H. C. *Science* **1993**, *261*, 888−891.
(18) Jarek, R. L.; Denson, S. C.; Shin, S. K. *J. Chem. Phys.* **1998**, *109*, 4258−4266. Jarek, R. L.; Shin, S. K. *J. Am. Chem. Soc.* **1997**, *119*, 10501−10508.
(19) Barthel, J.; Krienke, H.; Neueder, R.; Holovko, M. F. *Fluid Phase Equilib.* **2002**, *194*, 107−122. Weingartner, H.; Weiss, V. C.; Schroer, W. *J. Chem. Phys.* **2000**, *113*, 762−770.

10.1021/ja0602290 CCC: $33.50

Chart 1. Schematic Representation of the Novel [2+4] Cavitand-Containing Capsules[a]

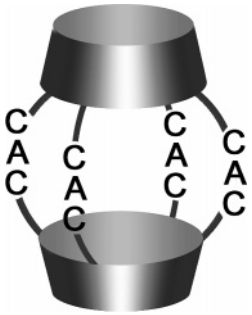

[a] A and C are singly charged anions and cations, respectively.

and a secondary valence denoted by a "coordination number".[20] This has been realized in a variety of anion receptors,[21] in which the coordination number of a singly charged anion can be up to nine.[20] In the case of anions, the secondary valence can be realized by electrostatic interactions,[22] anion−π interactions,[23] and hydrogen bonding.[20,21] These receptors can bind anions not only in noncompetitive solvents but also in polar competitive media and even in water.[21]

This paper deals with the first example of the use of triple-ion interactions for the construction of novel [2+4] cavitand-containing capsules (Chart 1) in methanol and water. The capsules are based on pyridinium−anion−pyridinium interactions, in which the anion has the coordination number two. Strong evidence for the capsule structure was obtained by in-source voltage-induced dissociation ESI-MS experiments. The interaction of the capsules with different guests was also studied.

Results and Discussion

Synthesis. For our studies, cavitands functionalized with four pyridiniummethyl substituents, containing different counterions, were used. Tetrakis(pyridiniummethyl)tetramethylcavitand tetrabromide **2** (X = Br)[24] was prepared by a slightly improved procedure starting from the corresponding tetrakis(bromomethyl)tetramethylcavitand **1**[25] (Scheme 2), using a mixture of chloroform/methanol instead of ethanol, giving less partially substituted compounds.

The known methanol-soluble cavitand **3**,[26] 1-(4-methylbenzyl)pyridinium salts **4**, and 1-(4-bromobenzyl)pyridinium bromide **5** were used as reference compounds (Chart 2). The nitrate, acetate, and tosylate salts of compounds **2** and **4** (X = NO_3, OAc, Tos) were prepared from the bromides **2** and **4**[27,28] (X = Br), respectively, using a column loaded with a Dowex anion-exchange resin functionalized with the appropriate anion.

Scheme 2. Synthesis of Cavitands **2**[a]

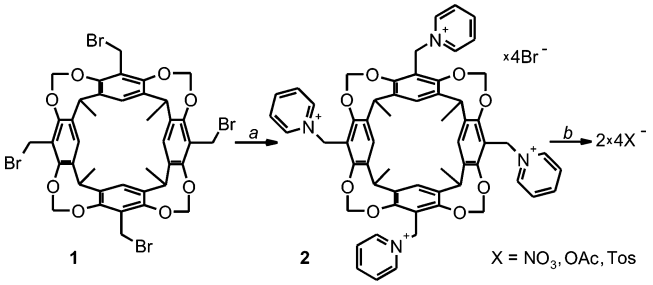

[a] Reagents and conditions: (a) pyridine, room temperature, in $CHCl_3$, after 12 h, in $CHCl_3$:MeOH (1:1); (b) Dowex X column.

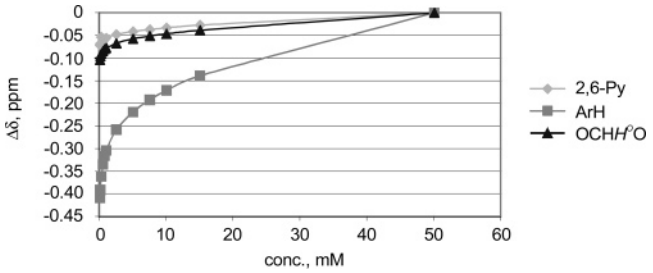

Figure 1. ^{1}H NMR shift differences observed upon dilution of **2**×4Br in methanol-d_4 (with respect to the shifts of **2**×4Br at 50 mM).

Chart 2. Reference Compounds

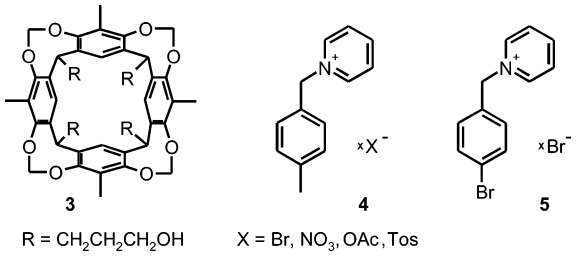

^{1}H NMR Spectroscopy. ^{1}H NMR dilution experiments of compounds **2** in methanol-d_4 show changes in the shifts of almost all the protons (up to ~0.4 ppm) upon varying the concentration from 0.1 to 50 mM (for example, see Figure 1). Since different types of protons experience shift changes upon dilution, different species and/or equilibria may be involved.

To understand this behavior, ^{1}H NMR dilution experiments were carried out with the reference pyridinium salts **4** (for an example, see Figure 2). The largest shift differences were observed for the 2,6-pyridinium, 2,6-(4-methylbenzyl), and methylene protons. The dilution data in Figure 2 cannot be fitted with a 1+1 model and represent at least two consecutive processes: the first process, with a K_a value of ~10^{2-3} M^{-1} (the first part of the curve), is followed by one or several interactions that have a lower affinity. From the literature it is known that pyridinium salts experience ion-pairing in solution,[29] to which the first observed process can be attributed. Since anions form coordination compounds[20] with π-electron-deficient aromatics including azaheterocycles (the coordination number

(20) Bowman-James, K. *Acc. Chem. Res.* **2005**, *38*, 671−678.
(21) For reviews on anion receptors, see: Kubik, S.; Reyheller, C.; Stuwe, S. *J. Inclusion Phenom. Macrocycl. Chem.* **2005**, *52*, 137−187. Gale, P. A. *Coord. Chem. Rev.* **2003**, *240*, 191−221 and other reviews in the same issue. Fitzmaurice, R. J.; Kyne, G. M.; Douheret, D.; Kilburn, J. D. *J. Chem. Soc., Perkin Trans. 1* **2002**, 841−864. Beer, P. D.; Gale, P. A. *Angew. Chem., Int. Ed.* **2001**, *40*, 487−516. Antonisse, M. M. G.; Reinhoudt, D. N. *Chem. Commun.* **1998**, 443−448.
(22) Worm, K.; Schmidtchen, F. P. *Angew. Chem., Int. Ed. Engl.* **1995**, *34*, 65−66.
(23) Rosokha, Y. S.; Lindeman, S. V.; Rosokha, S. V.; Kochi, J. K. *Angew. Chem., Int. Ed.* **2004**, *43*, 4650−4652.
(24) Grote Gansey, M. H. B.; Bakker, F. K. G.; Feiters, M. C.; Geurts, H. P. M.; Verboom, W.; Reinhoudt, D. N. *Tetrahedron Lett.* **1998**, *39*, 5447−5450. Middel, O.; Verboom, W.; Reinhoudt, D. N. *Eur. J. Org. Chem.* **2002**, 2587−2597.
(25) Sorrell, T. N.; Pigge, F. C. *J. Org. Chem.* **1993**, *58*, 784−785.
(26) Mezo, A. R.; Sherman, J. C. *J. Org. Chem.* **1998**, *63*, 6824−6829. Pirondini, L.; Bonifazi, D.; Menozzi, E.; Wegelius, E.; Rissanen, K.; Massera, C.; Dalcanale, E. *Eur. J. Org. Chem.* **2001**, 2311−2320.
(27) Katritzky, A. R.; Watson, C. H.; Degaszafran, Z.; Eyler, J. R. *J. Am. Chem. Soc.* **1990**, *112*, 2471−2478.
(28) Shpan'ko, I. V.; Korostylev, A. P.; Rusu, L. N. *J. Org. Chem. USSR (Engl. Transl.)* **1984**, *20*, 1715−1723.
(29) Larsen, J. W.; Edwards, A. G.; Dobi, P. *J. Am. Chem. Soc.* **1980**, *102*, 6780−6783. Hemmes, P.; Costanzo, J. N.; Jordan, F. *J. Phys. Chem.* **1978**, *82*, 387−391. Chuck, R. J.; Randall, E. W. *Spectrochim. Acta* **1966**, *22*, 221−226.

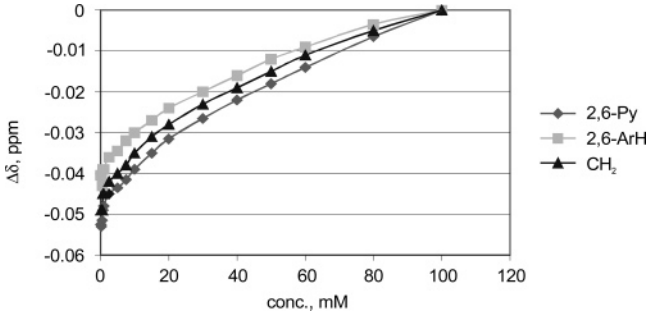

Figure 2. ^{1}H NMR shift differences observed upon dilution of **4**×Br in methanol-d_4 (with respect to the shifts of **4**×Br at 100 mM).

is two to four)[23] and the formation of pyridinium−anion−pyridinium triple ions has been detected electrochemically,[15,30] the further shift changes in the ^{1}H NMR spectrum can be explained by the formation of triple ions and, probably, higher aggregates.

To study the ability of the cavity of the cavitand to include an anion in methanol as a solvent, a ^{1}H NMR titration of reference cavitand **3** with Bu_4NBr was carried out. From the change of the shifts of the CH at the bottom rim and the inner proton of the OCH_2O-linker of the cavitand scaffold, a binding constant of 3−70 M^{-1} was determined by nonlinear fitting (ion-pairing of 0−10^3 M^{-1} of Bu_4NBr was taken into account in the fitting model).

From the experiments with the reference compounds, it can be concluded that the shifts observed upon dilution of compound **2** (Figure 1) are caused by several processes: inclusion of the anion into the cavity, ion-pairing of the anion with the pyridinium moiety, triple-ion formation, and, probably, the formation of higher aggregates.

The position of the anions with respect to the pyridinium cation **2** was determined with NOESY NMR in the cases of **2**×4Tos (see the Supporting Information) and **2**×4OAc. Cross-peaks between the α- and β-pyridinium protons and the 2,6-protons of tosylate or the acetate methyl group show that the counterions form contact ion-pairs with the pyridiniums in solution (10 mM in methanol-d_4). The organic substituents at the sulfonic or carboxylic groups, respectively, are located close to the pyridinium rings. It allows the conclusion that, in addition to electrostatic interactions between the pyridinium nitrogens and anions, additional CH−π interactions of the hydrogens of the anions with the pyridinium rings take place. The absence of cross-peaks between the α- and β-pyridinium protons and tosylate in **4**×Tos (40 mM in methanol-d_4) in the NOESY NMR spectrum recorded under the same conditions is an indication of the lower degree of association of this reference compound in solution.

Due to the complexity of the different processes, as well as the fast exchange between the species in solution, ^{1}H NMR spectroscopy cannot be used for a detailed study. Therefore, ESI-MS was used since it gives the opportunity to differentiate between the species present and to study the processes involved in more detail.

Basic ESI-MS Experiments. ESI-MS spectra of a methanolic solution of **2**×4Br at different voltages are shown in Figure 3.[31] Three intense signals that correspond to a complex of

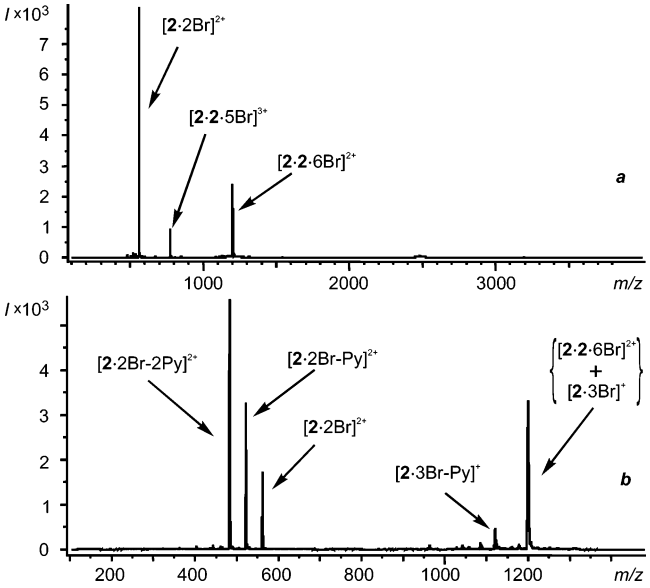

Figure 3. ESI-MS spectrum of a 0.5 mM solution of **2**×4Br in methanol (voltages: capillary, 2500 V; ring lens, 30 V; orifice 1, 2 V; orifice 2, 2 V (a) and 15 V (b)).

tetrakis(pyridiniummethyl)tetramethylcavitand **2** with two bromides ([**2**·2Br]$^{2+}$) and associates containing two molecules of **2** with five or six anions ([**2**·**2**·5Br]$^{3+}$ and [**2**·**2**·6Br]$^{2+}$, respectively) are present in the standard spectrum (Figure 3a). Upon increase of the concentration of **2**×4Br, the intensity of the signals of the associates grows and then, after about 1.5 mM (at standard voltage settings), decreases due to suppression.[32] Using nano ESI-MS (continuous-flow mode) diminishes the influence of the suppression,[33] and the increase of the intensity of the signal of the higher associates was observed until at least 5 mM **2**×4Br.

The associates [**2**·**2**·5Br]$^{3+}$ and [**2**·**2**·6Br]$^{2+}$ were also observed in the ESI-MS spectrum of a solution of **2**×4Br in water. However, the intensities of the signals of the complexes are about 5 times lower than in methanol (at the same concentrations), probably due to the competitive influence of water. It is striking that, both in water and in methanol, higher aggregates are not observed.

For a better understanding of the behavior of anion−pyridinium complexes in the gas phase, experiments were carried out with reference compounds **4**. Figure 4a,b shows the ESI-MS spectra of 1 mM solutions of **4**×Br^- in the positive and negative modes, respectively. Both spectra contain triple ions [**4**·Br·**4**]$^+$ and [Br·**4**·Br]$^-$, as well as the higher aggregates [**4**·(Br·**4**)$_n$]$^+$ and [Br·(**4**·Br)$_n$]$^-$ (n = 1−6).[34] A similar aggregation behavior was observed for the other anions: nitrate, acetate, and tosylate. The coordination number of the anions[20] in the observed complexes is two. Higher coordination is not realized

(30) Hojo, M.; Nagai, H.; Hagiwara, M.; Imai, Y. *Anal. Chem.* **1987**, *59*, 1770−1774.

(31) To keep a clear difference between compounds and ESI-MS signals, they are represented with the use of × and · symbols (for example, **2**×4Br and [**2**·2Br]$^{2+}$), respectively.

(32) Oshovsky, G. V.; Verboom, W.; Fokkens, R. H.; Reinhoudt, D. N. *Chem. Eur. J.* **2004**, *10*, 2739−2748.

(33) Due to the formation of much smaller droplets in nano ESI-MS in comparison with standard ESI-MS, the movement of large molecules from a solution to the gas phase is not more significantly diffusion limited. It causes a higher intensity of signals of large molecules in the nano mode and gives a more realistic representation of the species in solution.

(34) A similar aggregation of pyridinium salts was observed: Yoneda, M.; Tanizaki, K.; Tsujimoto, K.; Ohashi, M. *Org. Mass Spectrom.* **1993**, *28*, 693−698. Alfassi, Z. B.; Huie, R. E.; Milman, B. L.; Neta, P. *Anal. Bioanal. Chem.* **2003**, *377*, 159−164.

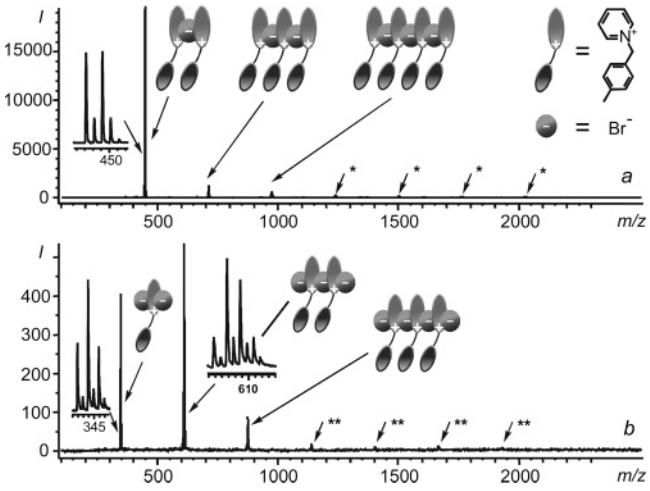

Figure 4. ESI-MS spectra in positive (a) and negative (b) modes of a 1 mM solution of **4**×Br^- in methanol: *, $[\mathbf{4}\cdot(Br\cdot\mathbf{4})_n]^+$, **, $[Br\cdot(\mathbf{4}\cdot Br)_n]^-$ (n = 3−6).

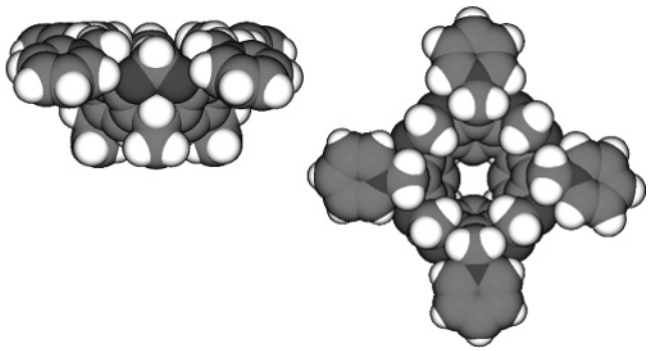

Figure 5. Optimized structure of the tetrakis(pyridiniummethyl)tetramethylcavitand **2**: side (left) and top (right) views.

due to steric hindrance caused by the benzylic substituents and, probably, an additional anion−π interaction with the benzene ring of the substituent.[23] The gas-phase observations correspond with the aggregation behavior observed in solution.[35]

For the interpretation of the basic mass spectrometric data, the preferential conformation of the tetrakis(pyridiniummethyl)-tetramethylcavitand **2** in the gas phase was determined by molecular modeling using Quanta/CHARMm (Figure 5). Cavitand **2** looks like an open flower in the gas phase, with the pyridinium moieties bent outward.[36]

Theoretically, there are two possible ways for anions to associate with cavitand **2** in the complex represented by the $[\mathbf{2}\cdot 2Br]^{2+}$ signal: either two anions are ion-paired with the pyridinium moieties or one anion is located inside the cavity and the second one is ion-paired. Steric hindrance and the position of two neighboring pyridinium groups in cavitand **2** do not allow intramolecular pyridinium−anion−pyridinium triple-ion formation.

(35) Due to the different volatility and stability of the species observed in the mass spectrum, ESI-MS cannot be used for the quantification of the solution processes (see ref 32).

(36) The X-ray crystal structures of **2**×4Br and **2**×$4NO_3$ confirm the open flower structure of cation **2**. Nevertheless, due to packing forces and the domination of CH anion above electrostatic interactions in the solid state, none of the interactions observed in solution and in the gas phase, giving rise to capsule formation, takes place in the solid state. In the case of the structurally related calix[4]arene tetrasulfonate, Atwood et al. noted a perturbation of supramolecular structures present in solution due to the crystallization process (for a review, see: Atwood, J. L.; Barbour, L. J.; Hardie, M. J.; Raston, C. L. *Coord. Chem. Rev.* **2001**, *222*, 3−32).

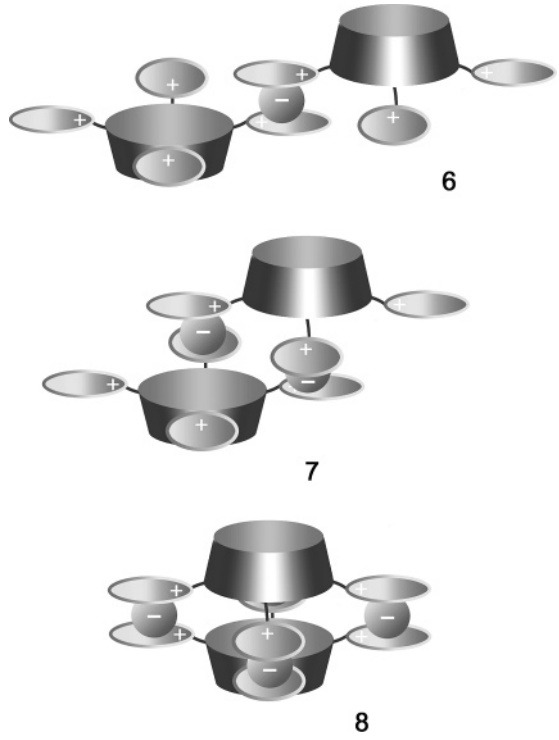

Figure 6. Possible ways of triple-ion aggregation of cavitands **2** [tetrakis-(pyridiniummethyl)tetramethylcavitand **2** is shown schematically].

Similar to the simple pyridinium salts (Figure 4), triple-ion interactions can bring together two cavitands **2**. There are three possible triple-ion associates (**6**−**8**) that are not significantly sterically hindered (Figure 6). Two of them contain one or two triple-ion linkers and form associates **6** and **7**, respectively. In the third case, [2+4] capsule **8** is formed by four triple-ion interactions.

The characteristic difference between the mass spectra of the bromides of cavitand **2** and reference compound **4** is the absence of significant signals of associates containing more than two organic molecules in the first case. It indicates that the formation of higher associates is very unfavorable or impossible. This points to the formation of capsule **8**, since its further triple-ion association is impossible due to the absence of free pyridinium moieties (or pyridinium−anion ion-pairs). The formation of higher aggregates of **8** via cation−anion−cation−anion−cation interactions can be excluded for steric reasons. In the cases of the complexes **6** and **7**, subsequent transformations into trimers, tetramers, etc. will be possible via triple-ion interactions in which free pyridinium moieties are involved.

The complexation of anions by reference cavitand **3** (vide supra) suggests the possible encapsulation of anions by capsule **8**. A complex of one or two bromides within the triple-ion capsule $[\mathbf{2}\cdot\mathbf{2}\cdot 4Br]^{4+}$ would explain the $[\mathbf{2}\cdot\mathbf{2}\cdot 5Br]^{3+}$ and $[\mathbf{2}\cdot\mathbf{2}\cdot 6Br]^{2+}$ signals. The structure of the complex represented by the $[\mathbf{2}\cdot\mathbf{2}\cdot 5Br]^{3+}$ signal (Scheme 3) can correspond not only to a capsule containing one anion (anion@**8**) but also to hemicapsule **9**, which encapsulates two anions and exists in solution in equilibrium with a capsule containing two anions (2anions@**8**, $[\mathbf{2}\cdot\mathbf{2}\cdot 6Br]^{2+}$). To distinguish the isomers of $[\mathbf{2}\cdot\mathbf{2}\cdot 5Br]^{3+}$ and to obtain more structural information about the $[\mathbf{2}\cdot\mathbf{2}\cdot 6Br]^{2+}$ capsule, in-source voltage-induced dissociation experiments were carried out.

Scheme 3. Possible Structures of Anionic Complexes of the Capsule and Hemicapsule[a]

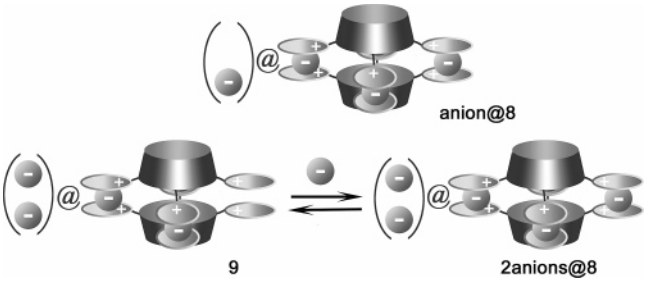

[a] Cavitand **2** is shown schematically.

Scheme 4. Possible Pyridinium Units Present in Complexes **6**, **7**, Capsule **8**, and their Associates with Anions

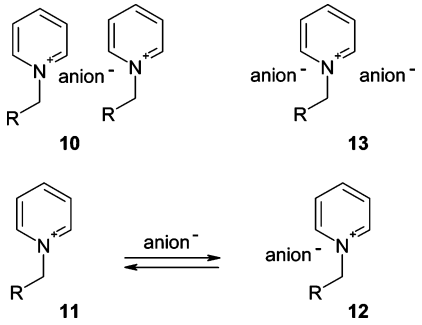

In-Source Voltage-Induced Dissociation Experiments. Mass spectrometry is a powerful tool not only for monitoring supramolecular interactions in solution[37] but also for the elucidation of the structure of supramolecular aggregates due to a different stability and gas-phase transformation of complexed and noncomplexed species.[38,39] In-source voltage-induced fragmentation/dissociation experiments,[39,40] realized by changes of the different voltages of an ESI mass spectrometer, were used to obtain evidence for the structure of the capsule and other complexes observed in the mass spectrum. In this study, the influence of varying the orifice and ring lens voltages was studied.[41] It is known that the orifice voltage causes in-source collision-induced dissociation.[39,40] Less is known about the effect of the ring lens voltage. Hinderling et al.[42] found, in the case of organometallic complexes, a different fragmentation compared to that caused by collision-induced dissociation.[43]

Complexes **6**, **7**, and capsule **8** have different types of (un)complexed pyridinium groups. Capsule **8** contains only triple-ion pyridinium−anion−pyridinium moieties **10**. In the complexes **6** and **7**, in addition to the triple-ion unit **10**, also methylenepyridinium cation **11** is present. The latter one is in equilibrium with contact ion-pair **12** (Scheme 4). Theoretically, in dimers of type **6** and **7** (complexed with several anions), the presence of anion−pyridinium−anion triple ion **13** is also possible. However, this type of pyridinium triple ions is much weaker than the pyridinium−anion−pyridinium units **10**. For example, Hojo et al.[15,30] reported that, in a conductometric study of pyridinium salts, the formation of pyridinium$^+(X^-)_2$-type species could not be observed at all, whereas (pyridinium$^+)_2X^-$ species were easily found in acetonitrile ($X^- = Cl^-$, Br^-).

Scheme 5. Gas-Phase Transformation of the Methylenepyridinium Cation: Cleavage of the C−N Bond

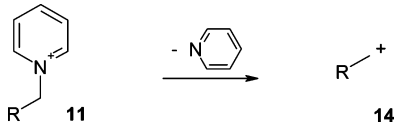

The different voltage-induced transformations of the complex fragments **10**−**13** in the gas phase were used to obtain additional evidence for the structure of the triple-ion [2+4] capsule **8**.

In the case of the ESI-MS spectrum of **2**×4Br, increasing the orifice 2 voltage[44] from 2 to 15 V causes fragmentations, which is clearly visible by comparing parts a and b of Figure 3.[45] The [**2**·2Br]$^{2+}$ complex at *m*/*z* 560 experiences loss of only one or two pyridines (Figure 3b), to give the [**2**·2Br−Py]$^{2+}$ and [**2**·2Br−2Py]$^{2+}$ complexes, respectively (Scheme 5). Ion-pairing stabilizes pyridinium cations.[38] For example, Schalley et al.[38] found that non-ion-paired substituted dibenzyl viologen is so unstable that, irrespective of the ionization conditions, the non-ion-paired cation was not detected in the mass spectrum. However, the viologen dication stabilized by ion-pairing is clearly observed in the spectrum as the most intense signal. It is well known that the non-ion-paired pyridinium cations **11** display the fragmentation shown in Scheme 5,[27,38,46] but no cleavage of the pyridinium cations from the ion-pairs takes place.[47] Since loss of three pyridines from the [**2**·2Br]$^{2+}$ complex does not take place, both anions are ion-paired with pyridiniums (unit **12**). This means that the other possible structure, in which one anion is ion-paired and the second one is included inside the cavity, can be excluded.

The [**2**·**2**·6Br]$^{2+}$ signal at *m*/*z* 1201 (Figure 3b) shows a much higher stability; nevertheless, increasing an orifice voltage (for example, 20 V, Figure 7b) does cause fragmentation of the triple-ion capsule [**2**·**2**·6Br]$^{2+}$ complex 2anions@**8**. It splits symmetrically to two [**2**·3Br]$^+$ cations.[48] The [**2**·**2**·6Br]$^{2+}$ and [**2**·3Br]$^+$ complexes have the same *m*/*z* but a different charge and isotopic contribution (due to the presence of six and three Br atoms, respectively), which allows them to be easily distinguished (Figure 7). The [**2**·3Br]$^+$ complex loses pyridine,

(37) Daniel, J. M.; Friess, S. D.; Rajagopalan, S.; Wendt, S.; Zenobi, R. *Int. J. Mass Spectrom.* **2002**, *216*, 1−27. Ganem, B.; Henion, J. D. *Bioorg. Med. Chem.* **2003**, *11*, 311−314. Schalley, C. A. *Int. J. Mass Spectrom.* **2000**, *194*, 11−39.
(38) Schalley, C. A.; Verhaelen, C.; Klarner, F. G.; Hahn, U.; Vogtle, F. *Angew. Chem., Int. Ed.* **2005**, *44*, 477−480.
(39) Gabelica, V.; De Pauw, E. *Mass Spectrom. Rev.* **2005**, *24*, 566−587.
(40) Bure, C.; Lange, C. *Curr. Org. Chem.* **2003**, *7*, 1613−1624.
(41) For details about the orifice and ring lens parts of an ESI mass spectrometer, see ref 39.
(42) Hinderling, C.; Feichtinger, D.; Plattner, D. A.; Chen, P. *J. Am. Chem. Soc.* **1997**, *119*, 10793−10804.
(43) The difference might be caused by the different design of the orifice and ring lens parts of the mass spectrometer resulting in the release of the excess energy of the ions via self-dissociation instead of collision-induced cleavage.
(44) Orifice 1 and orifice 2 voltages have a similar influence on the fragmentation. Nevertheless, due to the proximity of orifice 1 to the spray source, it also influences the movement of the species from droplets to the gas phase. It causes an increase of the intensity of the signals in the resulting spectrum, as well as the appearance of several additional signals that correspond to complexes of **2** with a different number of anions. To avoid the influence of this variable on the interpretation of the results, only the effect of orifice 2 voltage variations on the composition of the gas-phase mixture is shown in this paper.
(45) The influence of the gradual increase of the orifice 2 voltage is shown in the Supporting Information.
(46) Gabelica, V.; De Pauw, E.; Karas, M. *Int. J. Mass Spectrom.* **2004**, *231*, 189−195. Naban-Maillet, J.; Lesage, D.; Bossee, A.; Gimbert, Y.; Sztaray, J.; Vekey, K.; Tabet, J. C. *J. Mass Spectrom.* **2005**, *40*, 1−8.
(47) Recently, we have found that applying extremely drastic conditions cleaves the pyridinium cation from the contact ion-pair in capsules based on multivalent electrostatic interactions. In the case of pyridinium cations, the almost complete cleavage of pyridine takes place by 60 V (orifice 1 voltage). In the case of the pyridinium contact ion-pairs, the cleavage only begins at 100 V and is not complete even at 225 V.
(48) A similar dissociation of triple ions to ions and ion-pairs has been reported in an ESI-MS CID study of solutions of pyridinium-containing salts: Milman, B. L. *Rapid Commun. Mass Spectrom.* **2003**, *17*, 1344−1349.

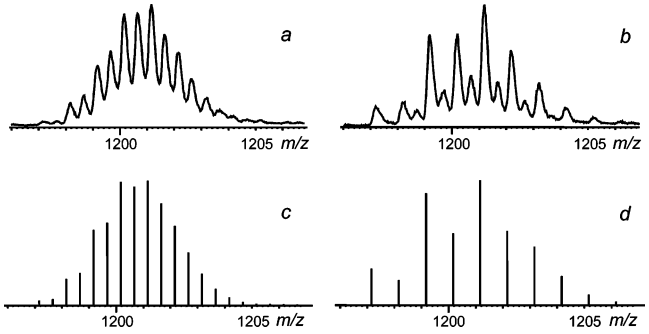

Figure 7. Example of the orifice voltage-induced fragmentation of capsule complex $[\mathbf{2}\cdot\mathbf{2}\cdot 6\mathrm{Br}]^{2+}$. (a) Initial complex. (b) Changes of the signal at increased orifice 2 voltage (20 V); two complexes are present, $[\mathbf{2}\cdot\mathbf{2}\cdot 6\mathrm{Br}]^{2+}$ and $[\mathbf{2}\cdot 3\mathrm{Br}]^{+}$. (c,d) The calculated isotopic patterns of $[\mathbf{2}\cdot\mathbf{2}\cdot 6\mathrm{Br}]^{2+}$ and $[\mathbf{2}\cdot 3\mathrm{Br}]^{+}$, respectively.

resulting in the appearance of the $[\mathbf{2}\cdot 3\mathrm{Br}-\mathrm{Py}]^{+}$ signal. This is in contrast to the $[\mathbf{2}\cdot\mathbf{2}\cdot 6\mathrm{Br}]^{2+}$ complex. The nonexistence of signals of $[\mathbf{2}\cdot\mathbf{2}\cdot 6\mathrm{Br}-n\mathrm{Py}]^{2+}$ ($n = 1, 2$) indicates the absence of pyridinium cations of type **11** in the structure of the $[\mathbf{2}\cdot\mathbf{2}\cdot 6\mathrm{Br}]^{2+}$ complex, because *non-ion-paired* methylenepyridinium cations should have been cleaved under these conditions (Scheme 5). This gives further evidence for the structure of the triple-ion capsule **8**. The encapsulation of two anions into the capsule **8** (2anions@**8**) is confirmed by the high stability of the $[\mathbf{2}\cdot\mathbf{2}\cdot 6\mathrm{Br}]^{2+}$ signal, since no collision loss of one or two bromides is observed.

The $[\mathbf{2}\cdot\mathbf{2}\cdot 5\mathrm{Br}]^{3+}$ signal disappears upon increase of the orifice voltage. However, instead of the loss of pyridine giving $[\mathbf{2}\cdot\mathbf{2}\cdot 5\mathrm{Br}-\mathrm{Py}]^{3+}$, the $[\mathbf{2}\cdot\mathbf{2}\cdot 5\mathrm{Br}]^{3+}$ complex breaks into the $[\mathbf{2}\cdot 2\mathrm{Br}]^{2+}$ and $[\mathbf{2}\cdot 3\mathrm{Br}]^{+}$ complexes. It allows the conclusion that its structure is very similar to that of the $[\mathbf{2}\cdot\mathbf{2}\cdot 6\mathrm{Br}]^{2+}$ capsule, but, due to its lower stability, it could rather correspond to hemicapsule **9** than to capsule anion@**8**.

Upon increase of the ring lens voltage, in the ESI-MS spectrum of $\mathbf{2}\times 4\mathrm{Br}$ a significant decrease of the intensity of the $[\mathbf{2}\cdot 2\mathrm{Br}]^{2+}$ signal was observed, probably due to deprotonation[49] of the benzylic pyridinium cation **11**.[50] The intensity of the $[\mathbf{2}\cdot\mathbf{2}\cdot 6\mathrm{Br}]^{2+}$ and $[\mathbf{2}\cdot\mathbf{2}\cdot 5\mathrm{Br}]^{3+}$ signals is much less sensitive to ring lens voltage changes. Experiments with reference compound **5** were carried out to compare the sensitivity of the signals of the benzylic pyridinium cation **11** and triple ions **10** to changes of the ring lens voltage. At a very low ring lens voltage (5 V), the observed intensity of the signal of the cation $\mathbf{5}^{+}$ is more than 15 times larger than that of the triple ion $[\mathbf{5}\cdot\mathrm{Br}\cdot\mathbf{5}]^{+}$ (Figure 8a). Upon increase of the ring lens voltage (30 V), the intensity of the signal of $\mathbf{5}^{+}$ drops more than 2 orders of magnitude, but the signal of the triple ion $[\mathbf{5}\cdot\mathrm{Br}\cdot\mathbf{5}]^{+}$ decreases[48] only 2 times and becomes the most intense signal in the spectrum (Figure 8b).[51] The higher stability of triple-ion complexes **10** in comparison with methylenepyridinium cations **11** is probably caused by the decreased acidity of the former due to the complexation.

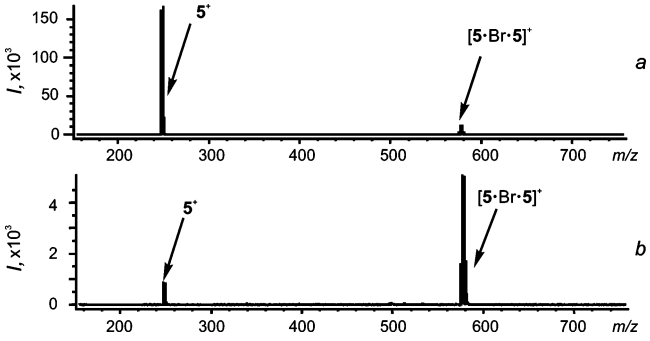

Figure 8. ESI-MS spectra of a 1 mM solution of $\mathbf{5}\times\mathrm{Br}$ in methanol (flow rate, 12.5 μL/min; capillary voltage, 2500 V; orifice 1 and 2 voltages, 2 V; ring lens voltage, 5 V (a) and 30 V (b)).

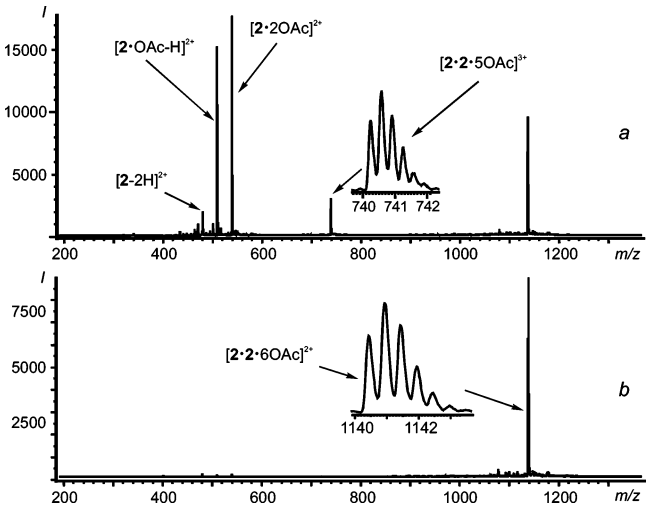

Figure 9. Continuous-flow nano ESI-MS spectrum of a 5 mM $\mathbf{2}\times 4\mathrm{OAc}$ solution in methanol (voltages: capillary, 2500 V; orifices 1 and 2, 5 V; ring lens, 20 V (a) and 30 V (b)).

Methylenepyridinium cations **11** are much more sensitive to increase of the ring lens voltage than triple ions **10** (vide supra). Hence, a high voltage stability of the $[\mathbf{2}\cdot\mathbf{2}\cdot 6\mathrm{Br}]^{2+}$ capsule indicates the absence of benzylic pyridinium units **11** in its structure. The $[\mathbf{2}\cdot\mathbf{2}\cdot 5\mathrm{Br}]^{3+}$ signal could rather correspond to the hemicapsule **9** than to dimers of type **6** and **7** (complexed with several anions). Despite the presence of pyridinium cations **11** in its structure, their deprotonation is less easy due to shielding of the protons by the second cavitand **2**.

Ring lens voltage experiments with $\mathbf{2}\times 4\mathrm{NO_3}$ exhibited for the most part a similar behavior. However, in the case of $\mathbf{2}\times 4\mathrm{OAc}$, a different behavior was observed. Figure 9a shows the continuous-flow nano ESI-MS spectrum of a 5 mM solution of $\mathbf{2}\times 4\mathrm{OAc}$ in methanol in the positive mode. The spectrum displays the signals of the $[\mathbf{2}\cdot\mathbf{2}\cdot 6\mathrm{OAc}]^{2+}$ capsule and the $[\mathbf{2}\cdot\mathbf{2}\cdot 5\mathrm{OAc}]^{3+}$ hemicapsule at *m*/*z* 1141 and 741, respectively. The signal of the complex of tetrapyridiniumcavitand **2** with two acetate anions ($[\mathbf{2}\cdot 2\mathrm{OAc}]^{2+}$) at *m*/*z* 540 is accompanied by two signals that are formed by cleavage of acetic acid from the ion-pairs of type **12**.[52] Upon increase of the voltage, only the signal of the $[\mathbf{2}\cdot\mathbf{2}\cdot 6\mathrm{OAc}]^{2+}$ capsule remains in the spectrum, and its intensity is almost unchanged (Figure 9b). Such a high stability of the capsule is explained by the absence of contact ion-pair

(49) Methylenepyridinium cation **14** has a high CH acidity due to the Coulombic effect of the positive charge and the resonance delocalization effects of the aromatic ring. Zhang, X. M.; Bordwell, F. G.; Vanderpuy, M.; Fried, H. E. *J. Org. Chem.* **1993**, *58*, 3060−3066.

(50) At low ring lens voltage, $\mathbf{2}^{4+}$ and $[\mathbf{2}\cdot\mathrm{Br}]^{3+}$ signals are also present. But, due to lower stability of these cations, they experience easy deprotonation and, therefore, disappear upon increase of the voltage.

(51) Further increase of the ring lens voltage (45 V) leads to dissociation of $[\mathbf{5}\cdot\mathrm{Br}\cdot\mathbf{5}]^{+}$ to $\mathbf{5}^{+}$ and $[\mathbf{5}\cdot\mathrm{Br}]^{0}$, which causes a relative increase of the intensity of the $\mathbf{5}^{+}$ signal in comparison with that of the $[\mathbf{5}\cdot\mathrm{Br}\cdot\mathbf{5}]^{+}$ signal. However, the absolute intensity of both signals decreases.

(52) The similar cleavage of pyridinium-containing ion-pairs, namely loss of an anion accompanied by deprotonation (in total, loss of an acid), is considered in ref 48.

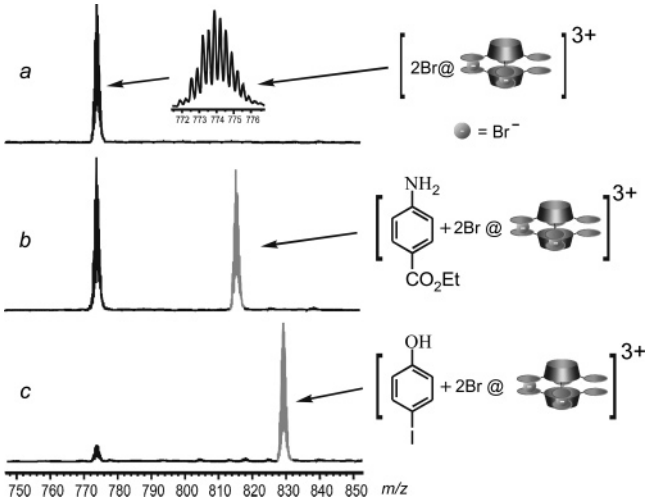

Figure 10. Continuous-flow nano ESI-MS spectra of a 5 mM solution of **2**×4Br in methanol (a), and upon addition of ethyl 4-aminobenzoate (b) or 4-iodophenol (c). In both cases, the resulting concentration of the guest is 40 mM.

moieties **12**, as well as effective shielding of the anions by pyridinium planes in the triple ions. A corresponding fragmentation of $[\mathbf{2}\cdot 2\mathrm{Br}]^{2+}$ and $[\mathbf{2}\cdot 2\mathrm{NO_3}]^{2+}$ is much less probable due to the much lower basicity of bromide and nitrate compared with acetate.

In the cases of **2**×4Br, **2**×4NO_3, and **2**×4OAc, the ESI-MS spectra exhibit a significant signal of a capsule containing two anions $[\mathbf{2}\cdot\mathbf{2}\cdot 6\mathrm{Anion}]^{2+}$ (corresponding with 2anions@**8** in Scheme 3). As expected, in the case of **2**×4Tos the cavity of the capsule has not enough space to accommodate two large tosylate anions. As a result, in the ESI-MS spectrum the $[\mathbf{2}\cdot\mathbf{2}\cdot 5\mathrm{Tos}]^{3+}$ signal, corresponding to a capsule with one guest molecule (as anion@**8** in Scheme 3), is intense and voltage-stable. The signal of the $[\mathbf{2}\cdot\mathbf{2}\cdot 6\mathrm{Tos}]^{2+}$ capsule (2anions@**8**) containing two big guests has a very low intensity and displays voltage instability.

From the different ESI-MS experiments, it can be concluded that the $[\mathbf{2}\cdot\mathbf{2}\cdot 6\mathrm{Anion}]^{2+}$ complex has a much higher stability than the other species present. The presence of methylenepyridinium cations and contact ion-pairs (**11** and **12**, respectively, in Scheme 4) can be excluded on the basis of the results with the reference compounds and the different fragmentation behavior of the noncapsule species. Hence, all these data point to the formation of a triple-ion [2+4] capsule with two anions (Br^-, NO_3^-, OAc^-) inside (2anions@**8** in Scheme 3). In the case of tosylate, due to its size, the capsule **8** contains only one anion.

Host−Guest Complexation. Upon addition of phenols or anilines to a solution of **2**×4X in methanol, the appearance of a new signal $[\mathrm{guest}\cdot\mathbf{2}\cdot\mathbf{2}\cdot 5\mathrm{X}]^{3+}$ ($X^- = Br^-$, NO_3^-) was observed in the mass spectra (Figure 10). The intensity of the signal of the $[\mathbf{2}\cdot\mathbf{2}\cdot 5\mathrm{X}]^{3+}$ hemicapsules (**9**) decreases. In the continuous-flow nano ESI-MS spectrum of a solution containing 5 mM **2**×4Br and 40 mM ethyl 4-aminobenzoate in methanol, the intensity of the two signals is almost the same (Figure 10b). In the case of 4-iodophenol, the $[\mathrm{guest}\cdot\mathbf{2}\cdot\mathbf{2}\cdot 5\mathrm{Br}]^{3+}$ signal becomes much more intense, while the signal of the $[\mathbf{2}\cdot\mathbf{2}\cdot 5\mathrm{Br}]^{3+}$ hemicapsule (**9**) almost disappears (Figure 10c). A moderate decrease (about 30%)[53] of the intensity of the signal of capsule

Scheme 6. Schematic Representation of the Host−Guest Complex Formation

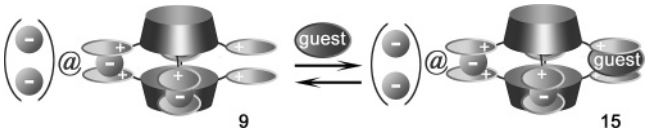

2anions@**8** was also observed upon guest addition, which is probably the result of its participation in an equilibrium with hemicapsule **9** (Scheme 3). Attempts to substitute encapsulated anions for guests that could form complexes inside the cavity of the cavitand, such as acetone, ethyl acetate, benzene, toluene, acetonitrile, etc.,[54] were not successful. It indicates a much higher affinity of the cavitand capsule toward anions than to neutral molecules in the competitive solvent methanol. It is in agreement with ^{1}H NMR observations in methanol-d_4: cavitands form complexes with anions[55] (vide supra), but in the spectra expected shift changes have not been observed upon the addition of neutral organic guests.

The position of the guest was deduced from ^{1}H NMR titration experiments. Upon addition of 4-iodophenol to a solution of **2**×4Br in methanol-d_4, a shift of the 4-pyridinium proton of **2** up to 0.075 ppm was observed, while no significant changes of the OC*H*^{i}H^{o}O-protons pointing into the cavity of **2** took place. From that, it can be concluded that the guest is positioned not in the cavity but between two pyridinium planes (Scheme 6). In addition, molecular modeling showed that ethyl 4-aminobenzoate is too large to be accommodated within the capsule. The formation of the novel type of capsule−guest complex **15** can be explained by $\pi-\pi$ and charge-transfer interactions[56] between the electron-deficient pyridinium rings and the electron-rich phenols or anilines. This type of interactions, where pyridinium binding sites, realized in viologen cyclophanes, bind substituted phenols and naphthols, has widely been used by Stoddart et al. to build catenanes, borromean rings, molecular machines, etc.[57] Upon further increase of the concentration of 4-iodophenol, the appearance of the $[\mathrm{guest}\cdot\mathrm{guest}\cdot\mathbf{2}\cdot\mathbf{2}\cdot 4\mathrm{Br}]^{3+}$ signal that could correspond to a capsule, in which net two anions of the walls are substituted for the guest, was observed.[58]

Monitoring the decrease of the intensity of $[\mathbf{2}\cdot\mathbf{2}\cdot 5\mathrm{Br}]^{3+}$ as a reference signal upon guest addition allows an estimation[35] of the relative capsule−guest affinity[32,59] (Chart 3). In general, 4-iodo-substituted phenol and aniline are the best guests. This can be explained by an additional interaction of iodine with protons of the methylene linker connecting pyridinium and cavitand.[60]

(53) A relative decrease in comparison with the sum of the intensities of the $[\mathrm{guest}\cdot\mathbf{2}\cdot\mathbf{2}\cdot 5\mathrm{Br}]^{3+}$ and $[\mathbf{2}\cdot\mathbf{2}\cdot 5\mathrm{Br}]^{3+}$ signals.
(54) Gui, X.; Sherman, J. C. *Chem. Commun.* **2001**, 2680−2681.
(55) Upon complexation of organic anions large ^{1}H NMR shifts (up to 5 ppm) have been observed: Oshovsky, G. V.; Verboom, W.; Reinhoudt, D. N. *Collect. Czech. Chem. Commun.* **2004**, *69*, 1137−1148.
(56) Meyer, E. A.; Castellano, R. K.; Diederich, F. *Angew. Chem., Int. Ed.* **2003**, *42*, 1210−1250. Mori, T.; Inoue, Y. *Angew. Chem., Int. Ed.* **2005**, *44*, 2582−2585.
(57) Cantrill, S. J.; Chichak, K. S.; Peters, A. J.; Stoddart, J. F. *Acc. Chem. Res.* **2005**, *38*, 1−9. Liu, Y.; Bonvallet, P. A.; Vignon, S. A.; Khan, S. I.; Stoddart, J. F. *Angew. Chem., Int. Ed.* **2005**, *44*, 3050−3055. Rowan, S. J.; Cantrill, S. J.; Cousins, G. R. L.; Sanders, J. K. M.; Stoddart, J. F. *Angew. Chem., Int. Ed.* **2002**, *41*, 898−952.
(58) Complexation at the outside of the capsule, as was shown by Schrader et al. in the case of 1:1 calix[4]arene capsules (see ref 12), is of minor value due to the negligibly low intensity of the $[\mathrm{guest}\cdot\mathbf{2}\cdot\mathbf{2}\cdot 6\mathrm{Br}]^{2+}$ signals of complexes that could correspond to a complex of a guest with the capsule containing four anionic walls and two anions inside (see 2anions@**8** in Scheme 3).
(59) Brady, P. A.; Sanders, J. K. M. *New J. Chem.* **1998**, *22*, 411−417.

Chart 3. Relative Guest Affinity toward the $[\mathbf{2}\cdot\mathbf{2}\cdot 5\mathrm{Br}]^{3+}$ Hemicapsule (**9**)

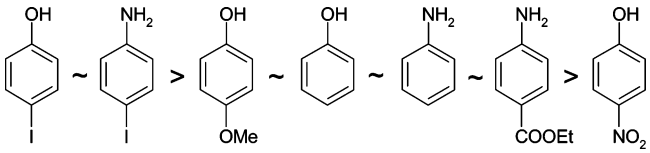

The complexes **15** represent a new type of unsymmetrical capsules, which has one pyridinium−guest−pyridinium wall and three pyridinium−anion−pyridinium walls.

Conclusions

For the first time, triple-ion interactions were used for the formation of capsules. The existence of the [2+4] cavitand-containing capsules, based on pyridinium−anion−pyridinium triple-ion interactions, was proven in the gas phase by ESI-MS. In addition, indications of the presence of the capsules in solution were obtained. A novel type of capsules is introduced in which one of the pyridinium−anion−pyridinium walls is replaced with a pyridinium−guest−pyridinium linker via equilibrium with the corresponding hemicapsule upon addition of a guest.

We feel that triple-ion interactions can be used, alone or together with other interactions, for the construction of different supramolecular architectures.

Experimental Section

The reagents used were purchased from Aldrich or Acros Chimica and used without further purification. All the reactions were performed under a dry argon atmosphere. All solvents were freshly distilled before use. Dry pyridine was obtained by distillation over calcium hydride. Melting points were measured using a Sanyo Gellenkamp melting point apparatus and are uncorrected. ^{1}H and ^{13}C NMR spectra were recorded on a Varian Unity Inova (300 MHz) spectrometer. Residual solvent protons were used as internal standard, and chemical shifts are given relative to tetramethylsilane (TMS). Ion-exchange resins were prepared from Dowex 550A OH anion-exchange resin, 25−35 mesh. Compounds **3**,[26] **4**×Br,[27,28] and **5**[27,61] were prepared similarly to the literature procedures (in the case of the compounds **4**×Br and **5**, acetone was used as a solvent instead of methanol, nitrobenzene, or nitromethane). The presence of water in the analytical samples was proven by ^{1}H NMR spectroscopy.

Quanta/CHARMm Calculations. The structural calculations were done using Quanta/CHARMm 2005 software. The tetrakis(pyridiniummethyl)tetramethylcavitand **2** preorganizes the pyridinium substituents in such a way that they are located in the corners of a square and point outside with angles of about 90° and 180° in the projection to the plane that is perpendicular to the C_4 axis of the molecule. The pyridinium rings are tilted only about 20° down from the plane. Due to steric hindrance caused by the oxygens of the cavitand scaffold and the protons of the CH_2N linker, the rotation around the C−N bond is restricted.

Determination of Binding Constants. K_a values (compound **3** with bromide) were determined by nonlinear fitting of calculated values (eqs 1−6) with experimental data obtained by ^{1}H NMR titration. The fitting program was based on Maple 8 software (Waterloo Maple Inc). The values of K_a, δ_{HG}, and δ_H were varied out until the best fitting of calculated with experimental data was obtained.

$$K_a = \frac{[HG]}{[H][G]} \quad (1)$$

$$K_{a,c} = \frac{[H_cG]}{[H][G_c]} \quad (2)$$

$$[G]_{tot} = [HG] + [H_cG] + [G] \quad (3)$$

$$[H]_{tot} = [HG] + [H] \quad (4)$$

$$[H_c]_{tot} = [H_cG] + [H_c] \quad (5)$$

$$\delta_{obs} = \chi_{HG}\delta_{HG} + \chi_H\delta_H \quad (6)$$

$[G]_{tot}$, $[H]_{tot}$, and $[H_c]_{tot}$ are total concentration of the guest, host, and competitor (tetrabutylammonium cation), respectively; $K_{a,c}$ is the binding constant of the anion with the competitor (several values varying from 0 to 10^3 M^{-1} were taken into the model); K_a is the binding constant of host **3** with bromide; [G], [H], $[H_c]$, [HG], and $[H_cG]$ are the concentrations of the guest, host **3**, competitor, the complexes of the host with the guest, and the complexes of the host with the competitor, respectively; χ_{HG} and χ_H are the mole fractions of the host−guest complex and host; δ_{obs} is the observed shift of the protons of the host; and δ_{HG} and δ_H are the shifts of protons of the host−guest complex and host, respectively. The error in the K_a values is about 5%.

ESI-MS. The ESI-MS experiments were carried out with a JEOL AccuTOF instrument. In the standard mode, the solutions were introduced at a flow rate of 12.5 μL/min. In the continuous-flow nano mode, the solutions were introduced with pressure (the flow rate set in the syringe pump was up to 400 nL/min) into fused-silica PicoTip emitters purchased from New Objective, Inc. The data were accumulated in the mass range 230−4000 *m*/*z* for 2 min. The standard spray conditions, unless otherwise specified, are as follow: capillary voltage, 2500 V; ring lens voltage, 30 V; orifice 1 voltage, 2 V; orifice 2 voltage, 2 V; orifice 1 temperature, 60 °C; temperature in the desolvation chamber, 120 °C; drying gas flow, 0.1−0.5 L/min; nebulizing gas flow, 0.5 L/min. For the characterization of compounds **2** and **4**, the most intense signals of the isotopic pattern observed are shown.

Tetrakis(pyridiniummethyl)tetramethylcavitand Tetrabromide 2×4Br. To a solution of tetrakis(bromomethyl)tetramethylcavitand[25] **1** (1.0 g, 1.04 mM) in chloroform (50 mL) was added pyridine (0.51 mL, 6.22 mM) dropwise. The reaction mixture was stirred for 12 h. To the suspension that formed was added methanol (50 mL), and the clear reaction mixture obtained was stirred for an additional 24 h. The reaction mixture was evaporated to dryness under vacuum. The product was purified twice by reprecipitation with diethyl ether from methanol. Yield 1.2 g (94%); mp > 300 °C (dec); ^{1}H NMR (5 mM, CD_3OD) δ 9.00 (d, 8 H, J = 6.2 Hz, α-pyridinium-H), 8.59 (t, 4 H, J = 7.7 Hz, γ-pyridinium-H), 8.11 (t, 8 H, J = 7.0 Hz, β-pyridinium-H), 7.89 (s, 4 H, cavArH), 6.30 (d, 4 H, J = 7.3 Hz, OCH*H*^{o}O), 5.81 (s, 8 H, $ArCH_2Py$), 4.97 (q, 4 H, J = 7.3 Hz, Ar_2CH), 4.77 + 4.75 (4 H + water, OCH*H*^{i}O), 1.89 (d, 12 H, J = 7.3 Hz, CH_3); ^{13}C NMR (50 mM, CD_3OD) δ 154.8, 147.4, 146.4, 141.6, 129.8, 126.4, 121.5, 101.7, 56.6, 33.5, 17.2; nano ESI-MS (5 mM, CH_3OH) *m*/*z* 560.15 ($[\mathbf{2}\cdot 2\mathrm{Br}]^{2+}$, calcd 560.12), 773.85 ($[\mathbf{2}\cdot\mathbf{2}\cdot 5\mathrm{Br}]^{3+}$, calcd 773.80), 1201.19 ($[\mathbf{2}\cdot\mathbf{2}\cdot 6\mathrm{Br}]^{2+}$, calcd 1201.16).

General Procedure for Ion Exchange. (1) Column Preparation. Dowex anion-exchange resin (~150 mL) was washed with methanol (1 L) and placed into a column (d = 25 mL) which had a small piece of wool above the stopcock at the bottom of the column. The column was flushed under pressure by methanol (1 L) and Q-water (2 L). Subsequently, it was washed by an aqueous solution of NaOH (1 N, 400 mL, mainly without pressure) and Q-water (1.5 L, with pressure). That was followed by washing with an aqueous solution of the salt

(60) For examples of CH−I interactions, see: Kobayashi, K.; Ishii, K.; Yamanaka, M. *Chem. Eur. J.* **2005**, *11*, 4725−4734. Laughrey, Z. R.; Gibb, C. L. D.; Senechal, T.; Gibb, B. C. *Chem. Eur. J.* **2003**, *9*, 130−139. Gibb, C. L. D.; Stevens, E. D.; Gibb, B. C. *J. Am. Chem. Soc.* **2001**, *123*, 5849−5850.
(61) Kröhnke, F.; Vogt, I. *Chem. Ber.* **1952**, *85*, 368.

chosen (mainly without pressure; 0.5 L of 1 N solutions of sodium nitrate, sodium acetate, and sodium tosylate in water were used for the preparation of Dowex NO_3, Dowex OAc, and Dowex Tos, respectively). To remove the excess of the salt, the column was washed with Q-water (2.5 L) and flushed with MeOH (300−500 mL, with pressure).

(2) Ion Exchange. A solution of compound **2**×4Br or **4**×Br (400 mg) in methanol (20 mL) was flushed into the Dowex Anion column without pressure. The column was washed with methanol (200 mL). The methanol solution was evaporated to dryness under vacuum without heating to give the **2**×4Anions or **4**×Anions in quantitative yields.

Tetrakis(pyridiniummethyl)tetramethylcavitand Tetranitrate 2×4NO$_3$: mp > 300 °C (dec); ^{1}H NMR (5 mM, CD_3OD) δ 8.97 (d, 8 H, J = 6.5 Hz, α-pyridinium-H), 8.59 (t, 4 H, J = 7.5 Hz, γ-pyridinium-H), 8.10 (t, 8 H, J = 6.8 Hz, β-pyridinium-H), 7.74 (s, 4 H, cavArH), 6.27 (d, 4 H, J = 7.3 Hz, OCHH^oO), 5.76 (s, 8 H, $ArCH_2Py$), 4.98 (q, 4 H, J = 7.3 Hz, Ar_2CH), 4.67 (d, 4 H, J = 7.3 Hz, OCHH^iO), 1.83 (d, 12 H, J = 7.3 Hz, CH_3); ^{13}C NMR (10 mM, CD_3OD) δ 154.9, 147.4, 146.4, 141.4, 129.7, 124.8, 121.8, 101.5, 56.3, 33.1, 24.2, 16.2; nano ESI-MS (5 mM, CH_3OH) m/z 542.17 ([**2**·2NO_3]$^{2+}$, calcd 542.19), 743.90 ([**2**·**2**·5NO_3]$^{3+}$, calcd 743.92), 1146.83 ([**2**·**2**·6NO_3]$^{2+}$, calcd 1146.87). Anal. Calcd for $C_{60}H_{56}N_8O_{20}$ + 3 H_2O (1263.2): C, 57.05; H, 4.95; N, 8.87. Found C, 57.21; H, 4.72; N, 8.75.

Tetrakis(pyridiniummethyl)tetramethylcavitand Tetraacetate 2×4OAc: mp > 200 °C (dec); ^{1}H NMR (5 mM, CD_3OD) δ 8.98 (d, 8 H, J = 5.9 Hz, α-pyridinium-H), 8.60 (t, 4 H, J = 7.5 Hz, γ-pyridinium-H), 8.11 (t, 8 H, J = 7.0 Hz, β-pyridinium-H), 7.68 (s, 4 H, cavArH), 6.29 (d, 4 H, J = 7.7 Hz, OCHH^oO), 5.77 (s, 8 H, $ArCH_2Py$), 4.98 (q, 4 H, J = 7.3 Hz, Ar_2CH), 4.74 (d, 4 H, J = 7.3 Hz, OCHH^iO), 1.80 + 1.82 (24 H, CH_3-cavitand + CH_3-acetate); ^{13}C NMR (25 mM, CD_3OD) δ 179.9, 154.9, 147.5, 146.4, 141.3, 129.8, 124.8, 121.9, 101.5, 56.2, 33.0, 24.2, 16.2; nano ESI-MS (5 mM, CH_3OH) m/z 1140.95 ([**2**·**2**·6OAc]$^{2+}$, calcd 1140.97). Anal. Calcd for $C_{68}H_{72}N_4O_{16}$ + 4.5 H_2O (1282.4): C, 63.69; H, 6.37; N, 4.37. Found C, 63.92; H, 6.40; N 4.11.

Tetrakis(pyridiniummethyl)tetramethylcavitand Tetratosylate 2×4Tos: mp 199−200 °C; ^{1}H NMR (5 mM, CD_3OD) δ 8.96 (d, 8 H, J = 5.5 Hz, α-pyridinium-H), 8.55 (t, 4 H, J = 7.7 Hz, γ-pyridinium-H), 8.07 (t, 8 H, J = 7.0 Hz, β-pyridinium-H), 7.69 + 7.71 (12 H, cavArH + α-tosylate-H), 7.22 (d, 8 H, J = 7.7 Hz, β-tosylate-H), 6.32 (d, 4 H, J = 7.7 Hz, OCHH^oO), 5.79 (s, 8 H, $ArCH_2Py$), 4.98 (q, 4 H, J = 7.3 Hz, Ar_2CH), 4.74 + 4.77 (4 H + water, OCH^iO), 2.35 (s, 12 H, CH_3-tosylate), 1.82 (d, 12 H, J = 7.3 Hz, CH_3-cavitand); ^{13}C NMR (20 mM, CD_3OD) δ 154.9, 147.3, 146.4, 143.9, 141.9, 141.3, 130.0, 129.7, 127.1, 124.9, 121.9, 101.7, 56.3, 33.0, 21.5, 16.3; nano ESI-MS (5 mM, CH_3OH) m/z 377.16 ([**2**·Tos]$^{3+}$, calcd 377.14), 651.23 ([**2**·2Tos]$^{2+}$, calcd 651.22), 925.95 ([**2**·**2**·5Tos]$^{3+}$, calcd 925.96). Anal. Calcd for $C_{88}H_{84}N_4O_{20}S_4$ + H_2O (1663.9): C, 63.52; H, 5.21; N, 3.37. Found C, 63.55; H, 5.33; N, 3.18.

1-(4-Methylbenzyl)pyridinium Nitrate 4×NO$_3$: transparent oil; ^{1}H NMR (10 mM, CD_3OD) δ 9.02 (d, 2 H, J = 5.5 Hz, α-pyridinium-H), 8.60 (t, 1 H, J = 7.7 Hz, γ-pyridinium-H), 8.10 (t, 2 H, J = 6.6 Hz, β-pyridinium-H), 7.38 (d, 2 H, J = 8.1 Hz, 2,6-benzyl-*H*), 7.29 (d, 2 H, J = 8.1 Hz, 3,5-benzyl-*H*), 5.79 (s, 2 H, $ArCH_2Py$), 2.36 (s, 6 H, CH_3); ESI-MS (1 mM, CH_3OH) m/z 430.24 ([**4**·NO_3·4]$^+$, calcd 430.21).

1-(4-Methylbenzyl)pyridinium Acetate 4×OAc: transparent, slightly yellowish oil, which easily turns brown upon heating or influence of light; ^{1}H NMR (10 mM, CD_3OD) δ 9.05 (d, 2 H, J = 5.4 Hz, α-pyridinium-H), 8.61 (t, 1 H, J = 7.5 Hz, γ-pyridinium-H), 8.12 (t, 2 H, J = 6.8 Hz, β-pyridinium-H), 7.40 (d, 2 H, J = 8.1 Hz, 2,6-benzyl-*H*), 7.30 (d, 2 H, J = 8.1 Hz, 3,5-benzyl-*H*), 5.80 (s, 2 H, $ArCH_2Py$), 2.36 (s, 3 H, CH_3-tosylate), 1.90 (s, 3 H, CH_3-acetate); ESI-MS (1 mM, CH_3OH) m/z 427.26 ([**4**·OAc·4]$^+$, calcd 427.24).

1-(4-Methylbenzyl)pyridinium Tosylate 4×Tos: transparent oil; ^{1}H NMR (10 mM, CD_3OD) δ 9.02 (d, 2 H, J = 5.6 Hz, α-pyridinium-H), 8.59 (t, 1 H, J = 7.6 Hz, γ-pyridinium-H), 8.10 (t, 2 H, J = 6.8 Hz, β-pyridinium-H), 7.70 (d, 2 H, J = 8.0 Hz, α-tosylate-H), 7.38 (d, 2 H, J = 8.4 Hz, 2,6-benzyl-*H*), 7.29 (d, 2 H, J = 8.4 Hz, 3,5-benzyl-*H*), 7.22 (d, 2 H, J = 8.0 Hz, β-tosylate-H), 5.78 (s, 2 H, $ArCH_2Py$), 2.36 (s, 6 H, 2 × CH_3); ESI-MS (1 mM, CH_3OH) m/z 539.23 ([**4**·Tos·4]$^+$, calcd 539.24).

Acknowledgment. The authors warmly thank Prof. Dr. N. M. M. Nibbering for the fruitful discussions on the mass spectrometry part. We are grateful to the Council for Chemical Sciences of The Netherlands Organization for Scientific Research (CW-NWO) for financial support.

Note Added after ASAP Publication. After this paper was published ASAP on March 23, 2006, corrections were made in the first sentence of ref 33 and in the Figure 8 caption. The corrected version was published ASAP on March 24, 2006.

Supporting Information Available: Influence of the gradual increase of the orifice 2 voltage on the ESI-MS spectrum of **2**×4Br and the NOESY NMR spectrum of **2**×4Tos. This material is available free of charge via the Internet at http://pubs.acs.org.

JA0602290